International Journal of Heat and Mass Transfer 54 (2011) 1187–1197

Contents lists available at ScienceDirect

International Journal of Heat and Mass Transfer

journal homepage: www.elsevier.com/locate/ijhmt

Thermodynamic optimization of fluidized catalytic cracking (FCC) units

J.A. Souza [a], J.V.C. Vargas [b,*], J.C. Ordonez [c], W.P. Martignoni [d], O.F. von Meien [e]

[a] Escola de Engenharia, FURG, Universidade Federal do Rio Grande, Av. Itália, Km 08 S/N, Campus Carreiros, 96201-900 Rio Grande, RS, Brazil
[b] Departamento de Engenharia Mecânica, UFPR, Universidade Federal do Paraná, CP 19011, 81531-990 Curitiba, PR, Brazil
[c] Department of Mechanical Engineering and Center for Advanced Power Systems, Florida State University, 2525 Pottsdamer St., Room 229, Tallahassee, FL 32310-6046, USA
[d] PETROBRAS S.A., AB-RE/TR/OT, Av. Chile, 65, Sala 2102, Rio de Janeiro, RJ 20031-912, Brazil
[e] PETROBRAS S.A., UN-RIO/ST/EISA, Av. Gen. Canabarro, 500, 5° andar, Maracanã, Rio de Janeiro, RJ 20271-900, Brazil

ARTICLE INFO

Article history:
Received 27 May 2010
Received in revised form 4 October 2010
Accepted 4 October 2010
Available online 2 December 2010

Keywords:
Fluidization
Petroleum
Reactor analysis
Computational chemistry
Exergetic analysis
Mathematical model

ABSTRACT

In this paper, a thermodynamic optimization procedure for FCC riser units has been developed. The formulation uses a 2D fluid flow and kinetic model to provide the necessary information for the optimization process. The thermodynamic analysis is based on the unit entropy generation minimization, i.e., the minimization of the destroyed exergy in the system. This kind of analysis has been widely used in power generation plants, with large benefits. It was verified that for any given catalyst mass flow rate, there exists an optimum value for the catalyst to oil mass flow rate ratio, COR, for maximum mass flow rate production of gasoline, or any other desired product. Next, the objective function (net exergy production rate) was maximized through the minimization of the destroyed exergy inside the FCC unit. The optimization was conducted with respect to the catalyst to oil ratio (COR). It is important to stress that all optima are sharp, i.e., for example with $H/D = 50$, the variation of $\widetilde{E}_{net}$ is greater than 50%, calculated from $(\widetilde{E}_{net,max} - \widetilde{E}_{net,min})/\widetilde{E}_{net,max}$ for $5 < COR < 25$. Based on the lack of second law analysis related works for FCC plants in the technical literature and in view of the potential gains suggested by the results, the authors believe that thermodynamic optimization could bring new insight in the quest for better FCC plants. Therefore, a low computational time tool is made available for simulation, control, design and optimization of FCC units.

1. Introduction

New renewable energy sources have been among the most important issues in the world energy scenario in the last three decades, since the 1973 oil crisis. The search for non-pollutant energy sources, preferably renewable, is currently a common concern of most countries in the world. Great effort has been made by the scientific community, and significant advances have been achieved in the last two decades. Clean and renewable energy sources [1] (e.g., solar, wind, ocean) are currently at a high level of development and most of them have been successfully added by several countries to the power grid as complementary energy sources. Alternative renewable biofuels [2] are also of great commercial interest and new bio-diesel production technologies are under development to obtain oil from rapeseed, soybean, algal and many others. It is expected that these new sources will eventually replace the use of fossil fuels (e.g., petroleum, coal, natural gas). However, fossil fuels are still the most important energy source in the world.

Petroleum has a major importance in this scenario because its sub-products are largely used as fuel source for the majority of all transportation vehicles (e.g., cars, trucks, trains.) and is also used for power generation in industries or distant and isolated locations. Currently there is no other fuel capable of replacing the use of petroleum fuels. In recent years, scientists agreed that the world petroleum reserves were expected to finish by the middle of the third millennium. However, it is now known that oil reserves will last much longer, but exploration will become increasingly more difficult and expensive, and for this reason, eventually becoming commercially unattractive. New brands of petroleum, probably heavier ones, will demand new technologies and refining facilities operating close to their maximum capacity.

The fluidized catalytic cracking (FCC) is currently the most important process used in the conversion of heavy petroleum fractions into light and commercially interesting products. The numerical simulation of the FCC process of a petroleum refinery has been performed by several authors who have proposed different mathematical models [3–5]. With the constant increase of computational capabilities, such models have become even more complex and with wider application. The different models address both fluid flow and cracking kinetics, varying from simple one phase and one-dimensional models to three-dimensional and three-phase models. Therefore, there is no common ground regarding the most adequate formulation for FCC risers modeling, and

* Corresponding author. Tel.: +55 41 3361 3307; fax: +55 41 3361 3129.
E-mail address: jvargas@demec.ufpr.br (J.V.C. Vargas).

0017-9310
doi:10.1016/j.ijheatmasstransfer.2010.10.034

Nomenclature

A	area (m^2)
C	lump concentration (k mol/m^3)
C_c	coke concentration (kg_{coke}/kg_{cat})
Cp	specific heat (kJ/kg K)
D	riser diameter (m)
ΔH	reaction enthalpy (kJ/kg)
E	activation energy (kJ/k mol)
$\dot{E}$	exergy rate (kJ/K s)
$\widetilde{E}$	dimensionless exergy rate
FCC	fluidized catalytic cracking
h_{gs}	gas–solid heat transfer coefficient (kJ/m^3 s K)
H	length of the riser in the flow direction (m)
K	pre-exponential kinetic constant (m^3/kg_{cat} s or m^6/k mol kg_{cat} s)
K^r	kinetic reaction constant (m^3/kg_{cat} s or m^6/k mol kg_{cat} s)
$\dot{m}$	mass flow (kg/s)
M	molar mass (kg/k mol)
n	reaction order
N	number of lumps
p	pressure (Pa)
q_i	model adjusting constants 3, 7, $i = 1, \ldots, 6$
Q	heat flux (kJ/s)
r, z	cylindrical coordinates (m)
R, Z	dimensionless cylindrical coordinates
$\overline{R}$	universal gas constant (kJ/k mol K)
Re	Reynolds number
s	specific entropy (kJ/kg K)
S	entropy (kJ/K)
t	time (s)
T	temperature (K)
v_r, v_z	fluid velocities (m/s)
V_r, V_z	dimensionless fluid velocities (m/s)
Y	mass fraction

Greek symbols

ε	bed porosity
φ	phase volume fraction
ϕ	deactivation function
μ	absolute viscosity (m^2/s)
θ	dimensionless temperature
ρ	fluid density (kg/m^3)
τ	dimensionless time
Ω	reaction term (k mol/m^3 s)
ξ	chemical exergy (kJ/kg)
$\bar{\xi}$	chemical exergy (kJ/mol)

Subscripts

0	reference state (T_0 = 293 K, P_0 = 1 bar)
ad	adsorption
cat	catalyst
coke	coke lump of the kinetic model
dest	destroyed
gas	gaseous phase
gen	generated
i, j	general use
in	input
fg	fuel gas lump of the kinetic model
gsl	gasoline lump of the kinetic model
lco	light cycle oil lump of the kinetic model
LPG	liquefied petroleum gas lump of the kinetic model
prod	products
reac	reaction
reg	regenerator
ve	volume element
vgo	gasoil lump of the kinetic model

Superscripts

b	bottom
c	cooling
i, j	counters for the lumps
in	input
k	grid volume index
r	reaction
t	top

advantages and drawbacks may be identified in each available model [6].

In the case of a model that strives for unit optimization, it is necessary to have a fast and sufficiently precise code that will be used to run several simulations (each one for a specific operating condition), searching for the best values for the input variables (mass concentrations, temperatures, etc.). This is a difficult balance (i.e., a fast and sufficiently precise model). However, according to Theologos and Markatos [3], the overall performance of the riser can be predicted by a one-dimensional mass, energy and chemical species balances what suggests that simplified models as in Han et al. [7] and Souza [8] may be precise enough to be used in an optimization process.

In that direction, several models for the optimization of FCC units have been proposed in the literature [7,9–11]. In all cases, the optimization was based on the maximization of the products production by the determination of the conditions (e.g., mass flows, inlet temperatures) for the maximum performance. This type of optimization methodology has produced good results in determining optimal operating conditions for maximum production, however it does not account for the thermodynamic losses that happen in the process, the amount of energy input necessary to produce the desired products, and the additional investment that results from them. Conversely, an exergy based optimization for the FCC unit allows for the determination of the optimal unit operating conditions for maximum products production, in a scenario where the consumption of energy and thermal losses due to heating the feedstock, cooling down the produced fuels and heat input for the chemical reactions inside the riser are taken into account in the calculations. Only one study was found in the literature that performs an exergy analysis applied to FCC units [12] which concluded that the key factors are to reduce the energy consumption of the regenerator, optimize the heat exchanging system and utilize the low temperature heat. However, no FCC riser optimization study was found in the literature based on the unit exergy destruction minimization.

Thermodynamic optimization is a successful methodology which has been applied for numerous engineering problems [13,14]. Its main concept is based on the minimization of the system generated entropy, i.e., minimization of system thermal losses. Power, propulsion, co-generation plants are application examples where the second law of thermodynamics has been used to minimize the heat losses and consequently maximize the thermal efficiency of the system, but the methodology is not usually applied to FCC units.

In FCC plants, all the energy necessary for the catalytic reactions is supplied by burning coke in a regenerator. Since the coke is considered a residue of the FCC plant, no attention is usually given to the possibility of maximizing the utilization of the energy potential that can be obtained from it. However, it should be emphasized

that all the excess energy consumed by the process could otherwise be used in other parts of the same unit, which in turn would represent a considerable operational cost reduction for the FCC plant. It is also important to point out that an exergy analysis applied to the FCC process is known to be challenging, since the physical properties (e.g., exergies, specific heats) of the petroleum fractions (lumps) are not easily obtained.

Based on the lack of second law analysis related works for FCC plants in the technical literature and in view of the potential gains, the authors believe that thermodynamic optimization could bring new insight in the quest for better FCC plants. Therefore, in the present work, a methodology for the thermodynamic optimization of FCC units is introduced. The determination of the physical properties of the petroleum fractions and the mathematical formulation used in the exergy calculations are described in detail. For the sake of generality and computational efficiency, a dimensionless mathematical model is developed and the results presented in normalized charts.

2. Mathematical model

Since the main scope of this work is the search for better FCC operating conditions (unit optimization), a simplified model with a two-dimensional fluid flow field combined with a 6-lump kinetic model to simulate the gasoil catalytic cracking process inside the riser reactor has been utilized. Two energy equations (catalyst and gasoil) are utilized to evaluate the temperature gradient between the two phases considered, i.e., the catalyst (solid) and the mixture gasoil/lift water vapor (gas). The model was published previously by the authors [15], and was adjusted with an available experimental data set [16], with 27 different operating conditions, 9 of which were used to determine appropriately placed fitting constants in the model equations, and then solving an inverse problem of parameter estimation [17] nine times. The other 18 known experimental operating conditions were used to validate the adjusted model with good quantitative and qualitative agreement. The model geometric and operating input parameters were obtained from a multipurpose plant located at SIX/PETROBRAS (Brazilian Oil Company), in São Mateus do Sul, Parana/Brazil [16] that was utilized to generate the experimental data set. The complete details of the model experimental validation are available in the literature [9,15].

Although the model has simplifying assumptions, the experimental validation demonstrated that the adjusted model captures the expected system physical trends, and is accurate enough, so that it could be used for FCC units design, simulation, control and optimization purposes. Therefore, in this work the model introduced previously by the authors [9,15] has been improved by the development of a dimensionless form of the riser equations and the addition of new second law based equations for the entire FCC unit, which are detailed next.

Fig. 1 shows the studied system, including the geometry and main simulation parameters. The geometry is defined by the length of the riser in the flow direction, H, and by the diameter of the riser, D. The dashed line defines the riser center line, where symmetry is noted. Regenerated catalyst, gasoil, and steam enter the system from the bottom of the riser; whereas the product lumps, the deactivated catalyst, and steam leave it from the top. The model assumes that all phases enter together through the bottom of the riser, which is an assumption used successfully by several authors [18,19].

Inside the riser, fluid flow is three-dimensional and multiphase. In this work, for simplicity, the problem is formulated as a two-dimensional well-mixed single phase flow, since the main objective is to quantify the output products, not the exact flow characteristics. The fluid is assumed to be incompressible, with uniform physical properties. The catalytic cracking reactions are modeled with a heterogeneous 6-lump model [20]. In spite of all simplifying assumptions, the two-dimensional fluid flow model consists of a more realistic and accurate model than the often used one-dimensional plug-flow models [19,21].

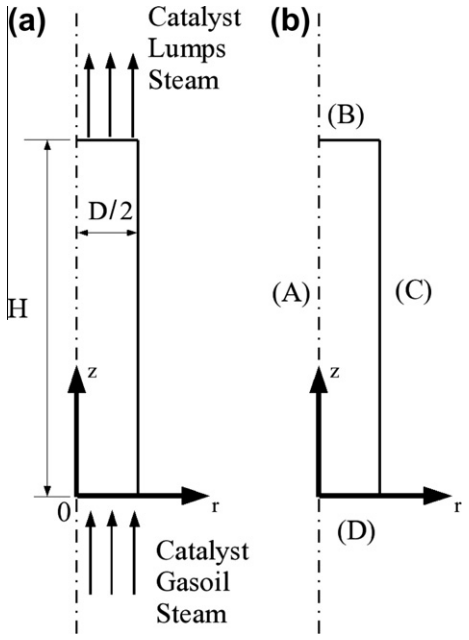

Fig. 1. Riser reactor: (a) geometry, (b) boundary conditions.

The FCC riser physics includes a number of variables with significant gradients in magnitude. While the bed porosity and mass fraction of the lumps components are close to unity, pressure has values with an order of magnitude of 10^5, whereas temperature has values with an order of magnitude of 10^2. Such gradients in the absolute values of the variables may bring numerical instabilities to reach convergence to the solution and in critical cases divergence might occur. In order to avoid possible numerical problems and to provide normalized results for general application to FCC risers of any size, the computational implementation of the mathematical model presented by Souza et al. [15] is herein non-dimensionalized, according to the description that follows.

2.1. Fluid dynamics model

The dimensionless variables are defined by

$$R = \frac{r}{D}; \quad Z = \frac{z}{D}, \tag{1}$$

$$V_r = \frac{v_r}{V_{in}}; \quad V_z = \frac{v_z}{V_{in}}, \tag{2}$$

$$\tau = \frac{V_{in}}{D}t, \tag{3}$$

$$P = \frac{p}{\rho V_{in}^2}, \tag{4}$$

$$\mathrm{Re} = \frac{\rho D V_{in}}{\mu}, \tag{5}$$

In Eqs. (1)–(5), r and z are the cylindrical coordinates (m), D the riser diameter (m), v the velocity (m s^{-1}), t the time (s), p the pressure (Pa) and R, Z, V, τ and P the respective dimensionless counterparts. The subscript in means input.

In Eqs. (4) and (5), ρ is the average mixture density (kg/m^3) and μ the average mixture absolute viscosity (Pa s). Both physical properties are kept constant during the simulation and calculated as

functions of the volumetric fraction of the particulate and gas phases as follows:

$$\rho = \varphi_{\text{gasoil}}\rho_{\text{gasoil}} + \varphi_{\text{st}}\rho_{\text{st}} + \varphi_{\text{cat}}\rho_{\text{cat}}, \tag{6}$$

$$\mu = \varepsilon\mu_{\text{gas}} + (1-\varepsilon)\mu_{\text{cat}} \quad \text{with} \quad \mu = \varepsilon\mu_{\text{gas}} + (1-\varepsilon)\mu_{\text{cat}}, \tag{7}$$

where φ is the phase volume fraction, ε the bed porosity, μ the weighted average between gas viscosity, μ_{gas}, and catalyst artificial viscosity in a fluid-like behavior, μ_{cat}, based on porosity, according to the model proposed by Miller and Gidaspow [22].

Using the defined dimensionless variables, the mass and momentum conservation equations are given by

$$\frac{\partial V_r}{\partial R} + \frac{V_r}{R} + \frac{\partial V_z}{\partial Z} = 0, \tag{8}$$

$$\frac{\partial V_r}{\partial \tau} + V_r\frac{\partial V_r}{\partial R} + V_z\frac{\partial V_r}{\partial Z} = -\frac{\partial P}{\partial R} + \frac{1}{\text{Re}}\left(\frac{\partial^2 V_r}{\partial R^2} + \frac{1}{R}\frac{\partial V_r}{\partial R} - \frac{V_r}{R^2} + \frac{\partial^2 V_r}{\partial Z^2}\right), \tag{9}$$

$$\frac{\partial V_z}{\partial \tau} + V_r\frac{\partial V_z}{\partial R} + V_z\frac{\partial V_z}{\partial Z} = -\frac{\partial P}{\partial Z} + \frac{1}{\text{Re}}\left(\frac{\partial^2 V_z}{\partial R^2} + \frac{1}{R}\frac{\partial V_z}{\partial R} + \frac{\partial^2 V_z}{\partial Z^2}\right). \tag{10}$$

2.2. Kinetic model

The reactions are modeled with the 6-lump model shown in Fig. 2. The six lumps are defined as vgo (non-converted gasoil lump in the riser), light cycle oil, gasoline, fuel gas, liquefied petroleum gas (LPG) and coke. The gasoil lump, vgo, should not be confused with the word gasoil which is commonly used to describe the total mass of oil, converted or not, flowing through the riser. In this sense, gasoil is actually the sum of all lumps including the vgo lump, which is the definition used in the present model.

The lump mass fraction (Y), which is already a dimensionless variable is defined as

$$Y_i^k = \frac{\dot{m}_i^k}{\dot{m}_{\text{gasoil}}^k} = \frac{C_i^k M_i v_z^k A^k}{\rho v_z^k A^k} = \frac{C_i^k M_i}{\rho}, \tag{11}$$

where M is the molecular weight (kg/k mol), A the riser cross-section area (m^2) and C the lump concentration (k mol/m^3). Subscript i, superscript k and subscript z refer to the lump number, a particular volume element in the mesh, and the dimensional direction, respectively.

The dimensionless species conservation equation for the lumps mass fractions is given by

$$\frac{\partial Y_i}{\partial \tau} + V_r\frac{\partial Y_i}{\partial R} + V_z\frac{\partial Y_i}{\partial Z} = \frac{M_i D}{\rho V_{\text{in}}}\Omega_i, \tag{12}$$

where in the present model, based on Fig. 2, with $N = 6$, the lumps are organized as $i = 1$: vgo; $i = 2$: light cycle oil; $i = 3$: gasoline; $i = 4$: LPG; $i = 5$: fuel gas, and $i = 6$: coke.

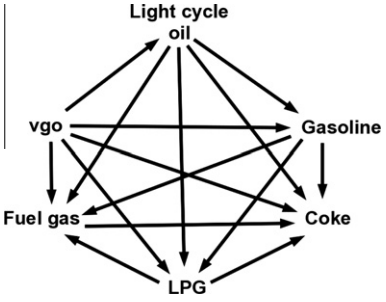

Fig. 2. Kinetic model scheme.

The reaction term in Eq. (12) is given by

$$\Omega_i = \left[\sum_{j=1}^{i-1} M_j K_{ji}^r \left(C_j^*\right)^{n_j} - \sum_{j=i+1}^{n} M_i K_{ij}^r \left(C_i^*\right)^{n_i}\right]\varphi(1-\varepsilon)\frac{\rho_{\text{cat}}}{M_i}, \tag{13}$$

$$C_i^* = \frac{1-\varepsilon}{\varepsilon}\rho_{\text{cat}} K_{\text{ad},i}^r C_i, \tag{14}$$

where N is the number of lumps, K the reaction constant, φ the catalyst deactivation function, n the reaction order and subscript ad means adsorption.

In Eq. (13), φ is the catalyst deactivation function given by

$$\varphi = e^{-406C_c}, \tag{15}$$

where C_c is the ratio between coke and catalyst mass (kg_{coke}/kg_{cat}).

In this kinetic model of Eq. (13) the vgo conversion reactions are second order while all other reactions are first order. The model is built with a set of 15 reaction constants which are experimentally obtained for a specific reaction temperature [20]. The relationship between these constants and the temperature is given by the Arrhenius Law, as follows:

$$K_{ij}^r = q_{j-1}K_{ij}e^{\left(\frac{-E_{ij}}{\overline{R}T_{\text{cat}}}\right)} \quad \text{for } i = 1 \quad \text{and} \quad j = 2,\ldots,6, \tag{16a}$$

$$K_{ij}^r = K_{ij}e^{\left(\frac{-E_{ij}}{\overline{R}T_{\text{cat}}}\right)} \quad \text{for } i = 2,\ldots,6, \tag{16b}$$

E is the activation energy (kJ/kg), $\overline{R}$ the universal gas constant (kJ/k mol K), and q_{j-1} are model adjusting constants determined experimentally, as reported by Souza et al. [9,15].

The catalytic reactions are endothermic, thus they consume part of the thermal energy available inside the riser reactor. This energy is taken from the catalyst which enters the riser at a high temperature (~993 K). Temperature is an important control variable in the catalytic conversion process and reactions only take place at a minimum reaction temperature. The catalyst helps to increase the reactions rates, but the temperature is the variable which rules these reactions. The energy exchange between the phases is another important issue. While the catalyst drops temperature along the riser, the gasoil heats up.

Furthermore, even though a one-phase model has been adopted in the fluid flow formulation, in order to include the energy balance between the phases (catalyst and gas), it was necessary to include in the model two energy equations. In the reaction (source) term of Eq. (12), the catalyst temperature is used to calculate the reaction kinetic constants, Eq. (16), while for the heat exchange between the particulate and gas phases, a second energy equation is necessary. Thus, the two energy equations, the particulate (catalyst) and the gas (gasoil plus steam), were written in dimensionless form as follows:

$$\left(\frac{\partial \theta_{\text{cat}}}{\partial \tau} + V_r\frac{\partial \theta_{\text{cat}}}{\partial R} + V_z\frac{\partial \theta_{\text{cat}}}{\partial Z}\right) = \widetilde{D}_{\text{cat}}\left[(\theta_{\text{cat}} - \theta_{\text{gas}})T_{\text{cat}}^{\text{in}} + \widetilde{\Delta}_{\text{vgo}} + \widetilde{\Delta}_{\text{coke}}\right], \tag{17}$$

$$\left(\frac{\partial \theta_{\text{gas}}}{\partial \tau} + V_r\frac{\partial \theta_{\text{gas}}}{\partial R} + V_z\frac{\partial \theta_{\text{gas}}}{\partial Z}\right) = \widetilde{D}_{\text{gas}}(\theta_{\text{gas}} - \theta_{\text{cat}}), \tag{18}$$

where the dimensionless variables are given by

$$\theta_i = \frac{T_i}{T_{\text{cat}}^{\text{in}}}, \tag{19}$$

$$\widetilde{D}_{\text{cat}} = \frac{Dh_{\text{gs}}}{\varphi_{\text{cat}}\rho_{\text{cat}}\text{Cp}_{\text{cat}}V_{\text{in}}T_{\text{cat}}^{\text{in}}},$$
$$\widetilde{D}_{\text{gas}} = \frac{Dh_{\text{gs}}}{\left(\varphi_{\text{gas}}\rho_{\text{gas}}\text{Cp}_{\text{gas}} + \varphi_{\text{st}}\rho_{\text{st}}\text{Cp}_{\text{st}}\right)V_{\text{in}}}, \tag{20}$$

$$\widetilde{\Delta}_{vgo} = \frac{-q_6 \Delta H_{vgo} \Omega_{vgo} M_{vgo}}{h_{gs}}, \quad \widetilde{\Delta}_{coke} = \frac{\Delta H_{coke} \Omega_{coke} M_{coke}}{h_{gs}}, \tag{21}$$

where i refers to a particular substance or location, Cp is the specific heat (kJ/(kg K)), ΔH the reaction enthalpy (kJ/kg), h_{gs} heat transfer coefficient (kJ/(m^3 K)), q_6 model adjusting constant determined experimentally, as reported by Souza et al. [9,15], and the subscripts are cat for catalyst, gas for gaseous phase, in for input and gs for gas–solid phases.

2.3. Boundary conditions

The computational domain and adopted boundary conditions are shown in Fig. 1(b), and written mathematically as follows:

$$A: \begin{cases} V_r = 0, \quad \frac{\partial V_z}{\partial R} = 0, \quad \frac{\partial P}{\partial R} = 0, \\ \frac{\partial \theta_{gas}}{\partial R} = \frac{\partial \theta_{cat}}{\partial R} = 0, \\ \frac{\partial Y_i}{\partial R} = 0, \end{cases} \tag{22}$$

$$B: V_r = 0, \quad \frac{\partial V_z}{\partial Z} = 0, \tag{23}$$

$$C: V_r = V_z = 0, \tag{24}$$

$$D: \begin{cases} V_r = 0, \quad V_z = 1, \quad P = P_{in}, \\ \theta_{vgo} = \theta_{vgo}^{in}, \quad \theta_{cat} = 1, \\ Y_{vgo} = 1, \quad Y_i = 0 \quad (i = 2 \text{ to } 6). \end{cases} \tag{25}$$

Eq. (25) requires the evaluation of some parameters from known input conditions. The parameters that need to be calculated are the input velocity V_{in}, the concentration of gasoil at the riser input section C_{vgo}, and the corrected input catalyst temperature T_{cat}. Those calculations are detailed in the work of Souza et al. [15].

3. Process optimization

The dimensional version of the model presented in Section 2 was validated through direct comparison with experimental data, as reported by Souza et al. [9,15]. In order to use the model as a tool for the optimization of an FCC unit, it is necessary the knowledge of the range of operating conditions of the unit. In this work, the range of operating conditions of an existing pilot unit [16] is utilized for all optimization runs. The conditions are

- Catalyst to oil ratio (COR): from 2 to 25.
- Catalyst input temperature (T_{cat}): from 953 to 993 K (680 to 720 °C).
- Gasoil input temperature (T_{gasoil}): from 483 to 493 K (210 to 220 °C).
- Riser height (H): from 10 to 50 D, where D is the riser diameter.

A steady state parametric analysis has been conducted within the above ranges. The operating conditions were varied within their operating limits and the unit response was analyzed. Table 1 summarizes the general characteristics of the pilot plant used in all simulations.

The effect of the catalyst to oil ratio (COR) on gasoil conversion is analyzed in Fig. 3. The graph shows the influence of the COR on the conversion of the heavy gasoil into lighter products of commercial interest. As seen in Fig. 3, the gasoil conversion rate increases with the increase of the COR. This is expected and also desired, because with the increase of the gasoil conversion, the production of gasoline and LPG also increase. For the gasoline, Fig. 3 shows a region where its conversion no longer increases as the catalyst to oil mass flow rates ratio increases, starting at $COR_{opt} \approx 15$. From that point and on, a slight decrease in gasoline conversion is observed, indicating the possibility of a maximum production of gasoline.

Table 1
General characteristics used in all simulations.

Feedstock		
Mass flow of gasoil (kg/h)	$\dot{m}_{gasoil}$	170*
Mass flow of steam (kg/h)	$\dot{m}_{st}$	5% of $\dot{m}_{gasoil}$
Riser input pressure (bar)	P_{in}	2.5
Physical parameters		
Catalyst density (kg/m^3)	ρ_{cat}	1400
Catalyst specific heat (kJ/kg K)	Cp_{cat}	1.09
Gasoil density (kg/m^3)	ρ_{gasoil}	26
Gasoil specific heat (kJ/kg K)	Cp_{gasoil}	2.67
Gasoil vaporization temperature (K)	T_{gasoil}^{vap}	733
Gasoil heat of vaporization (kJ/kg)	L_{gasoil}	155
Steam density (kg/m^3)	ρ_{st}	0.7
Steam specific heat (kJ/kg K)	Cp_{st}	4
Water heat of vaporization (kJ/kg)	L_w	2261
Catalyst input temperature (°C)	T_{cat}^{in}	680
Gasoil input temperature (°C)	T_{vgo}^{in}	210
Steam input temperature (°C)	T_{st}^{in}	210 (same as vgo)
Gaseous phase viscosity (Pa s)	μ	1.4×10^{-5}
Heat transfer coefficient between the phases (kJ/m^3 s K)	h_{gs}	1.0×10^{3}

* When not specified.

However, the conversion of gasoil into lighter products in an FCC unit should not be analyzed based only on the results of Fig. 3(a). The complementary analysis is based not only in the mass fraction conversion of gasoil into products, but also in the mass flow rates of each product. For that, it is recognized that any FCC unit presents a design constraint to operate at most with a given ceiling catalyst mass flow rate. Therefore, the conversion of gasoil into gasoline, for example, could be close to its maximum (~40%) with the gasoline mass flow rate being smaller than the maximum capacity of the unit, if $COR \approx 15$ is used.

Therefore, the optimization problem could be alternatively formulated by taking into account a given ceiling catalyst mass flow rate for the FCC unit. Accordingly, by varying the gasoil mass flow rate and fixing all other operating conditions, it results that COR could be optimized for maximum mass flow rate of a given product of interest (e.g., gasoline). In other words, the optimization problem objective function is the output mass flow rate of a product which should be maximized, for a fixed catalyst mass flow rate.

In this way, it is possible to explain why industrial units [23–25] in general operate with COR and gasoline conversion rates values close to 5% and 30%, respectively. The sole analysis of Fig. 3(a) leads to the conclusion that all units should operate with higher COR values than 5. However, Fig. 3(b) shows a simulation in which the catalyst mass flow rate is fixed at 600 kg h^{-1} (simulating a given limiting unit capacity). All other variables are set as shown in Table 1, except the gasoil mass flow rate, which was allowed to vary. According to Fig. 3(b), the maximum production of gasoline (in terms of mass flow rate) is obtained with a COR value close to 3. At this point, the gasoil conversion is around 25%, and more than 70% of the entire feedstock (gasoil) that enters the unit is not converted. For this reason this is probably not the ideal commercial operation point, i.e., gasoline mass flow rate is maximized at the

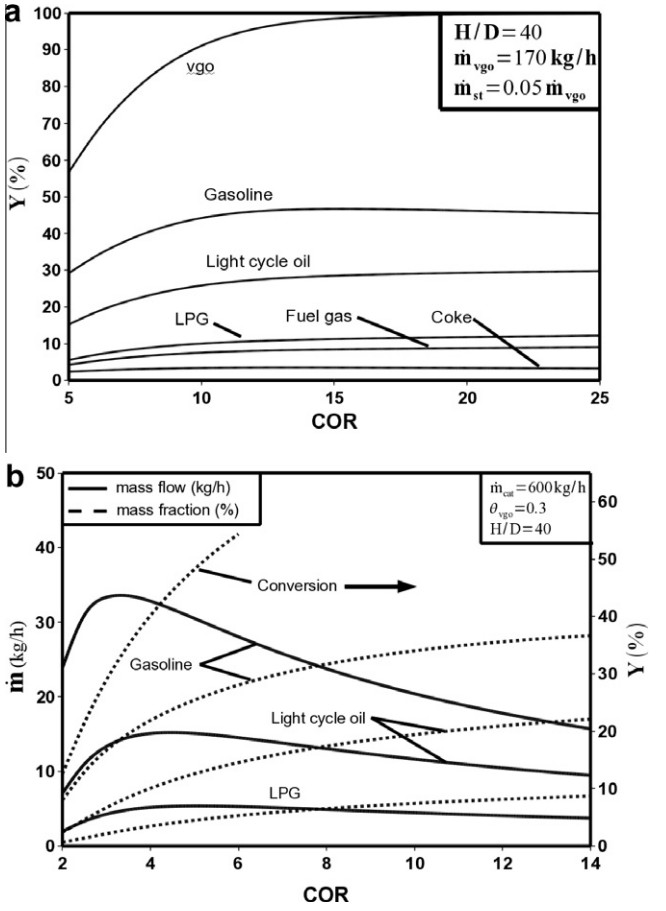

Fig. 3. (a) The effect of catalyst to oil mass flow rate ratio (COR) on gasoil conversion. (b) Gasoline, light cicle oil and LPG mass flow rates and mass fractions as functions of COR.

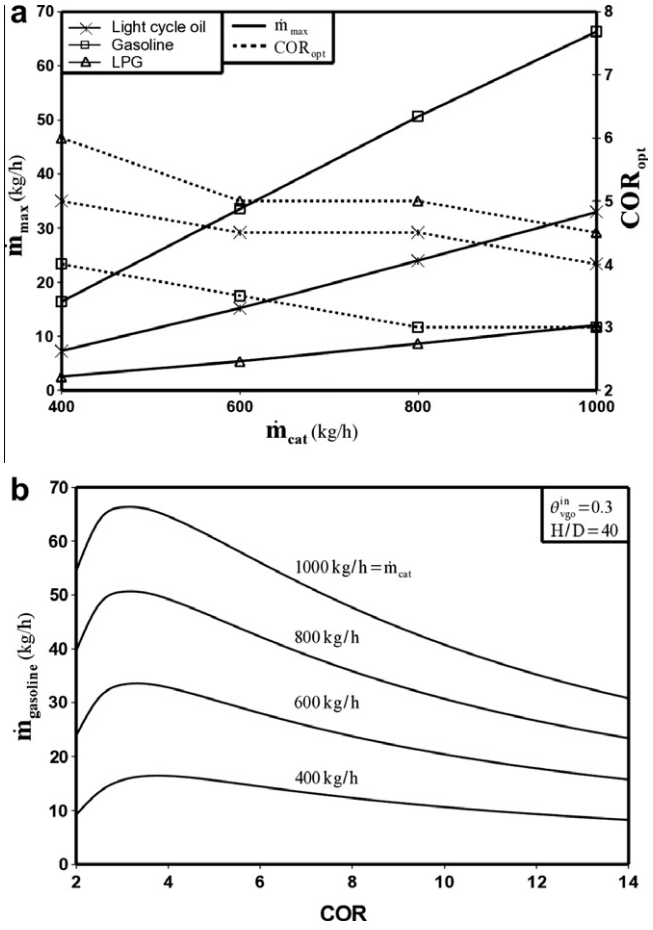

Fig. 4. (a) The effect of catalyst mass flow rate on $\dot{m}_{max}$ and COR_{opt}. (b) Gasoline mass conversion curves.

expense of gasoil wasting, which is not realistic. If the unit operated with COR ≈ 5, it would be close to the maximum production of LCO and LPG, and still with a large output gasoline mass flow rate, and in this case the total gasoil conversion is considerably higher than with COR ≈ 3.

In sum, although large gasoline mass flow rates are obtained with a COR value close to 3, large amounts of nonconverted gasoil need to be processed again, needing extra energy spending that otherwise would not be required if $COR_{opt} \approx 15$. Therefore, this analysis motivates the search for a methodology that takes into account the energy spending required by the process, i.e., thermodynamic optimization.

The analysis presented in Fig. 3(b) was repeated for constant catalyst mass flow rates of 400, 600, 800 and 1000 kg h^{-1}. The results are summarized in Fig. 4a in which it is seen that the COR_{opt} has a weak dependence on catalyst mass flow rate. For the gasoline lump, the COR_{opt} remains between 3 and 4 while the catalyst mass flow rate increased almost three times. For the other two lumps (LCO and LPG), the value of COR_{opt} is a little higher, but also "robust" with respect to the COR_{opt} variation.

Fig. 4(b) shows solely the optimization results obtained for the gasoline lump for several fixed catalyst mass flow rates. The gasoline production increases with the increase of the COR until it reaches a maximum value close to the point where COR ≈ 3. After this point, the gasoline mass flow rate decreases with the increase of COR. The maximum value for the gasoline mass flow rate was found to be close to 3 in all simulations, which is "robust" for a large range of $\dot{m}_{cat}$ values.

3.1. Thermodynamic optimization

The FCC unit has an important role in the oil refinery production. It is the unit where the conversion of heavy oil into light commercial products takes place. As a result, several FCC optimization studies can be found in the technical literature. However, most of such works are based only on the fluid dynamics and reaction kinetics of catalytic cracking, without exploring the unit's thermodynamic losses, i.e., the unit's entropy generation and, therefore the exergy destroyed in the process.

In this section, a methodology for the calculation of the total entropy generated by the FCC unit is introduced, followed by the process exergetic analysis. It is important to clarify that the study of the entropy generated by the FCC unit is performed after the model solution is available (velocities, products mass fractions and temperatures). Therefore the unit's total entropy generation is obtained by post processing the model solution data, and in this way quantifying the process thermodynamic losses. The entire procedure is described in the analysis that follows.

3.1.1. The entropy generation inside the riser

The total entropy generation rate in each volume element of the domain (riser interior), defined by the mesh selected to discretize the solution domain, is calculated using the volume element methodology introduced by Vargas et al. [26], as follows [13]:

$$\dot{S}_{gen,ve} = \frac{\partial S_{ve}}{\partial t} - \left(\sum_{i=1}^{N+2} \dot{m}_i s_i\right)_{inlet} + \left(\sum_{i=1}^{N+2} \dot{m}_i s_i\right)_{outlet} - \left(\frac{\dot{Q}}{T}\right), \qquad (26)$$

where $\dot{S}$ is the entropy rate (kW/K), s the specific entropy (kJ/(kg K)), N the number of lumps and $\dot{Q}/T$ the chemical reaction entropy generation inside the riser with $\dot{Q}$ the reaction enthalpy rate (ΔH_{reac}). The two extra lumps ($N+1$ and $N+2$) are used to account for the steam and catalyst contributions. Subscripts ve and gen mean volume element and generated, respectively.

The total entropy generation rate inside the riser reactor is therefore calculated by

$$\dot{S}_{gen} = \sum_{ve=1}^{n_{ve}} \dot{S}_{gen,ve}, \tag{27}$$

where n_{ve} is the total number of mesh volume elements.

Eqs. (27) and (26) must be applied to each one of the six lumps of the kinetic model. This calculation requires the determination of the specific entropies of each lump. Since these lumps are not components in isolation, the determination of its entropy is not an easy task. In this work, the main goal is to propose a thermodynamic optimization procedure for FCC risers, thus, for the sake of simplicity, the following assumptions were adopted: (i) all lumps, except the coke, have ideal gas behavior, and (ii) the specific reference entropy of each lump is assumed to be a hydrocarbon with similar molecular weight (Table 2).

The first assumption is a good approximation, since the pressure and velocities inside the riser are low and the gasoil is considered to enter the riser already vaporized. The second assumption is much more restrictive, but it is necessary because of the lack of information about the reference entropy of mixed fuels. If better information is available, then it will always be possible to reproduce the following numerical experiments with more accurate results. However, the main global and qualitative conclusions are expected not to be affected by such simplification.

For an ideal gas, the entropy change is calculated by [13]

$$\int_{S_0}^{S} dS = \int_{T_0}^{T} \frac{Cp}{T} dT - \int_{P_0}^{P} \frac{R}{P} dP, \tag{28}$$

where T_0, P_0 and S_0 are the reference states for the temperature, pressure and entropy respectively.

The evaluation of Eq. (28) requires the determination of the specific heat, Cp, as a function of the temperature. For the gas phase lumps (i = vgo, light cycle oil, gasoline, fuel gas and LPG) the specific heats were calculated by

$$Cp_i = C_1 + C_2 \left[\frac{\frac{C_3}{T}}{\sinh\left(\frac{C_3}{T}\right)} \right]^2 + C_4 \left[\frac{\frac{C_5}{T}}{\cosh\left(\frac{C_5}{T}\right)} \right]^2, \tag{29}$$

where the constants C_1, C_2, C_3, C_4 and C_5 were obtained from tabulated data [25].

For the coke, the specific heat of the graphite carbon curve was obtained from a correlation reported by Perry and Green [27], as follows:

$$Cp_{coke} = 2.673 + 0.002417\,T - \frac{1169900}{T^2}. \tag{30}$$

The specific heat of the catalyst was taken as constant (Table 1), since it is expected not to vary significantly within the riser temperature range of operation, and the following expression [27] was used to determine the specific heat of the steam:

$$Cp_{steam} = 0.807 \times 10^{-12} T^4 - 2.964 \times 10^{-9} T^4 + 4.152 \times 10^{-5} T^2 - 1.108 \times 10^{03} T + 4.08. \tag{31}$$

For the evaluation of Eq. (28), the reference values for the entropy ($S_{0,i}$) were obtained from tabulated data [27] at T_0 = 298.15 K and P_0 = 1 bar.

The total entropy generation rate inside the riser is evaluated by the sum of the generated entropy inside each one of the mesh volume elements. The calculation of the net entropy flow rate out of the volume element via mass flow ($\dot{m}_i s_i$) is schematically shown in Fig. 5. As it is observed, the entropy balance takes into account only the contributions in the z direction, by assuming the entropy fluxes in the r direction are negligible in comparison with the fluxes in the z direction, since the load flows from bottom to top of the riser.

The entropy flux of each lump, including the steam and catalyst, are calculated inside each volume element by

$$\dot{m}_i^b = Y_i^b \dot{m}_{gasoil}, \quad \dot{m}_i^t = Y_i^t \dot{m}_{gasoil}, \tag{32}$$

$$\dot{m}_{steam}^b = \varphi_{steam} \rho_{steam}^b v_z^b A^b, \quad \dot{m}_{steam}^t = \varphi_{steam} \rho_{steam}^t v_z^t A^t, \tag{33}$$

$$\dot{m}_{cat}^b = \varphi_{cat} \rho_{cat}^b v_z^b A^b, \quad \dot{m}_{cat}^t = \varphi_{cat} \rho_{cat}^t v_z^t A^t, \tag{34}$$

where i is the lump component, b and t the faces of the element, A the cross-section area of the volume element and v_z the velocity component in the z direction.

Combining Eqs. (26), (27), (32), (33), and (34) and assuming steady state operation, the total entropy generation rate inside the riser reactor is obtained by

$$\dot{S}_{gen} = \sum_{ve=1}^{n_{ve}} \left(\sum_{i=1}^{N+2} \left(\dot{m}_i^t s_i^t - \dot{m}_i^b s_i^b \right) - \frac{\Delta H_{reac}}{T} \right)_{ve}. \tag{35}$$

3.1.2. Exergetic analysis

The thermodynamic optimization of any kind of process can be understood as a procedure to quantify and minimize system fluid, thermal and chemical losses. These losses are directly associated with the system irreversibility and are normally associated with concentration and temperature gradients, fluid flow pressure drops, and for reaction systems, the heat generated or consumed during the chemical reactions. To minimize these losses means to minimize the irreversibilities, i.e., the exergy destroyed in the process in order to achieve maximum system thermodynamic performance.

A schematic representation of the exergetic analysis of a typical FCC unit is shown in Fig. 6. The analysis accounts for the exergy destruction inside the riser reactor and also by the main streams of catalyst and steam. The catalyst is assumed to operate in a

Table 2
Proposed lump × hydrocarbon equivalence and reference chemical exergy.

Lump		Hydrocarbon		Chemical exergy
Name	M (kg/k mol)	Name	M (kg/k mol)	$\bar{\xi}$ (kJ/mol)
vgo	422.800	*n*-Octadecane ($C_{18}H_{38}$)	254.500	11966.8
Light cycle oil	254.500	*n*-Octadecane ($C_{18}H_{38}$)	254.500	11966.8
Gasoline	114.200	*n*-Octane (C_8H_{18})	114.231	5418.60
LPG	44.100	Propane (C_3H_8)	44.097	2149.00
Fuel gas	16.040	Methane (CH_4)	16.043	830.20
Coke	0.000	Graphite carbon	–	410.500

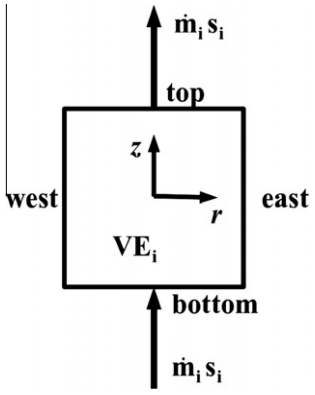

Fig. 5. Net entropy flow rate out of a mesh volume element via mass flow.

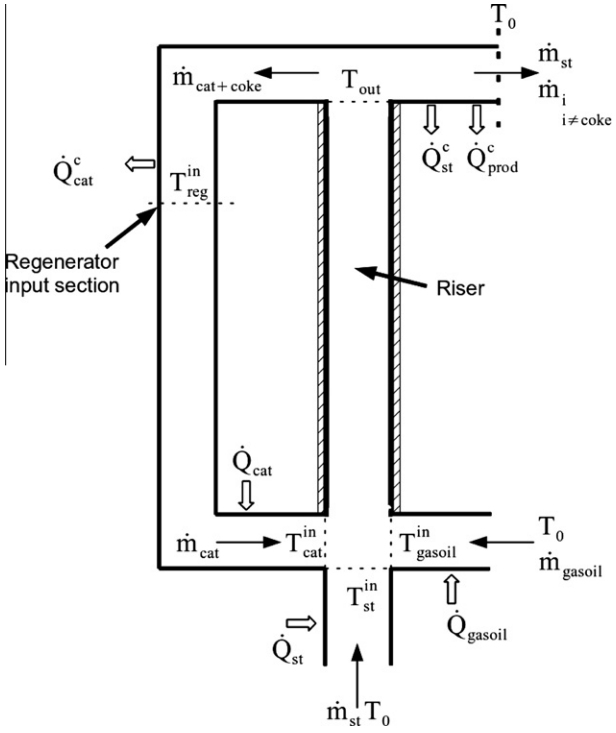

Fig. 6. FCC unit energy interactions and mass flow rates.

closed cycle inside the FCC unit whereas the gasoil and steam just pass through it. The gasoil and steam are considered to enter the unit (not the riser) at ambient temperature (20 °C). Before entering the riser these mass flow rates are heated up to the riser inlet temperature (~200 °C). The energy needed to heat those streams are represented in Fig. 6 by $\dot{Q}_{gasoil}$ and $\dot{Q}_{st}$.

The catalyst leaves the riser at temperature T_{out} and loses heat at the stripper and the pipes before entering the regenerator. This amount of lost energy is represented in Fig. 6 by $\dot{Q}^c_{cat}$. In the regenerator, the catalyst is re-heated up to its riser inlet temperature $\left(T^{in}_{cat} \sim 700\,^{\circ}C\right)$.

In the riser output section, the mass flow rate of the products and steam are at temperature T_{out}. These products leave the riser and pass by the fractioning section before being made available for consumption, therefore their final temperature will be the ambient temperature (T_0). In the present analysis, the destroyed exergy during the fractioning process considers only the energy lost by products cooling. The energy lost in this process is represented in Fig. 6 by $\dot{Q}^c_{prod}$ and $\dot{Q}^c_{st}$.

The total net exergy production rate in the process is therefore expressed as follows:

$$\dot{E}_{net} = \dot{E}_{prod} - \dot{E}_{dest} = \dot{E}_{prod} - \dot{E}_{cat} - \dot{E}_{gasoil} - \dot{E}_{st} - \dot{E}_{cooling} - T_0\dot{S}_{gen}. \quad (36)$$

The destroyed exergy ($\dot{E}_{dest}$) accounts for the system losses and must be subtracted from the total amount of exergy provided by the products. These products exergy is quantified by

$$\dot{E}_{prod} = (1 - Y_{vgo}) \sum_{\substack{i=1 \\ i\neq vgo}}^{N} \dot{m}_i \xi_i, \quad (37)$$

where ξ_i is the chemical exergy of the products at the reference temperature T_0.

In Eq. (37), the coke, which is actually a non-desired product, is also considered with available exergy. Since it is burned in the regenerator, and its energy is used to re-heat the catalyst, the coke chemical exergy must also be accounted by Eq. (37). The reference chemical exergies, at the reference temperature, are shown in Table 2.

The other terms in Eq. (36) represent the exergy destroyed during the process: $\dot{E}_{cat}$ is the destroyed exergy during the catalyst cooling, $\dot{E}_{gasoil}$ and $\dot{E}_{st}$ are the destroyed exergies due to heating of the gasoil and water, $\dot{E}_{cooling}$ is the exergy destroyed during the products and water steam cooling and $T_0\dot{S}_{gen}$ is the destroyed exergy of the mixture (gasoil, steam and catalyst) inside the riser reactor. The exergy destruction rates are quantified as follows:

$$\dot{E}_{cat} = \left(1 - \frac{T_0}{T_{out}}\right)\dot{Q}^c_{cat} + \left(1 - \frac{T_0}{T^{in}_{cat}}\right)\dot{Q}_{cat}, \quad (38)$$

$$\dot{E}_{gasoil} = \left(1 - \frac{T_0}{T^{in}_{gasoil}}\right)\dot{Q}_{gasoil}, \quad (39)$$

$$\dot{E}_{st} = \left(1 - \frac{T_0}{T^{in}_{st}}\right)\dot{Q}_{st}, \quad (40)$$

$$\dot{E}_{cooling} = \left(1 - \frac{T_0}{T_{out}}\right)\left(\dot{Q}^c_{st} + \dot{Q}^c_{prod}\right)., \quad (41)$$

The heat transfer rates in Eqs. (38)–(41) are described in detail in the Appendix A.

Finally, in the analysis, the exergy rates are nondimensionalized as follows:

$$\widetilde{E} = \frac{\dot{E}}{\dot{m}_{gasoil}\xi_{vgo}}, \quad (42)$$

where the subscript vgo refers to the gasoil lump of the kinetic model.

The first analysis herein considered explores the relationship between between $\widetilde{E}_{net}$ and the COR at different riser height/diameter ratios (H/D). Fig. 7 shows the results for COR values between 5 and 25. The gasoil mass flow rate is kept constant at 170 kg/h and the net exergy production rate is plotted for values of H/D equal to 10, 20, 30, 40 and 50. A maximum value for the net exergy ($\widetilde{E}_{net}$) is found for all curves at COR ~18. Here it is worth it to stress that all optima found are sharp, i.e., for example with H/D = 50, the variation of $\widetilde{E}_{net}$ is greater than 50%, calculated from $(\widetilde{E}_{net,max} - \widetilde{E}_{net,min})/\widetilde{E}_{net,max}$ for 5 < COR < 25.

In order to understand the maximum value for the net exergy production rate it is necessary to look at the individual contributions of each term of Eq. (36). These terms are plotted in Fig. 8 for the same operating condition of Fig. 7 for H/D = 10. It is clear that the maximum net exergy is mainly associated with the behavior of the $\widetilde{E}_{prod}$ and $\widetilde{E}_{cat}$ curves. For low values of COR, the $\widetilde{E}_{prod}$ increases monotonically with the increase of the conversion of gasoil.

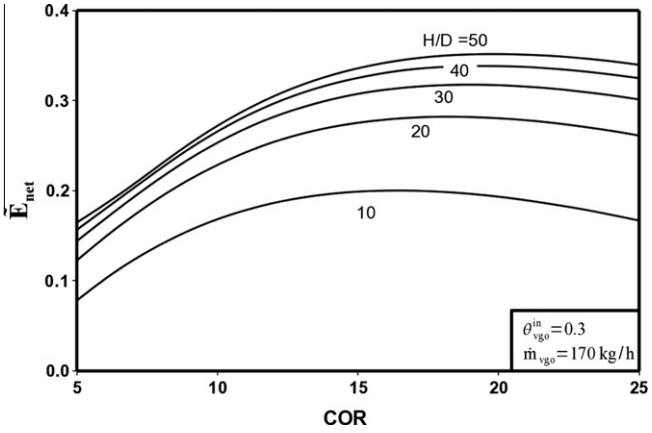

Fig. 7. Net exergy production rate as a function of COR and *H*/*D*.

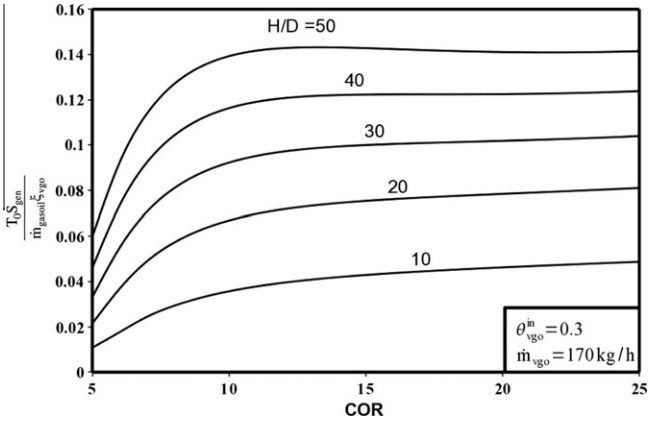

Fig. 9. Entropy generation rate inside the riser due to the chemical reactions.

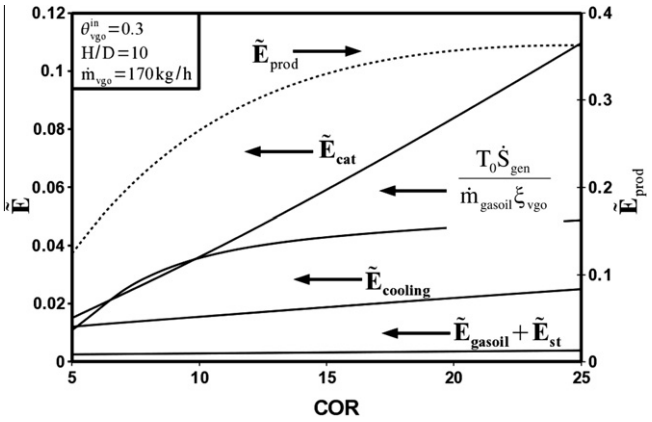

Fig. 8. FCC unit exergy rates components.

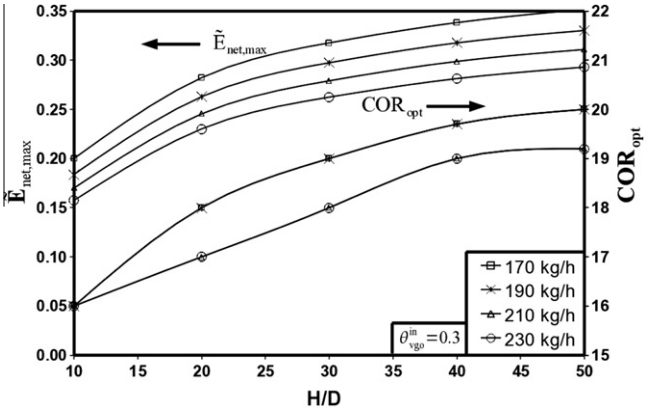

Fig. 10. Maximized net exergy production rate and optimal COR values.

This occurs for COR values below approximately 18. For higher values of COR, the gasoil conversion has already reached its plateau value and an increase in the COR will not increase conversion. Thus the products exergy will also stabilize as a constant value. The destroyed exergy during the heating of the catalyst is a linear function of the catalyst mass flow rate and for this reason, in this case where the gasoil mass flow rate is kept constant, the $\widetilde{E}_{cat}$ will always increase with the increase of the COR. The distinct behavior of these two exergy rates explains the existence of an optimal operating condition for the unit.

The entropy generation term $(T_0\dot{S}_{gen})/(\dot{m}_{gasoil}\xi_{vgo})$ has also an important contribution for the overall exergy balance. Its analysis is important for a better understanding of the chemical exergy destruction due to the catalytic cracking reactions. As seen in Fig. 9, the entropy generation rate varies significantly for COR values between 5 and 10. For higher values of COR, the entropy generation term no longer changes. This entropy generation rate inside the riser is due to the heat absorbed by the endothermic reactions. Such reactions will occur as long as gasoil is being consumed (converted in products). For low COR values, the conversion is low and the entropy generation rate will be low. Maximum conversion values are obtained with COR values equal or greater than 18, but actually for COR ~15, the gasoil conversion has already reached 95%. From this point and on, higher values of COR will not produce significantly higher conversion rates and consequently no significant increase in entropy generation rate as it is shown in Fig. 9.

In Fig. 10, the behavior of the maximum net exergy rate $(\widetilde{E}_{net,max})$ as a function of the *H*/*D* ratio and the gasoil mass flow rate is shown. The riser diameter and the inlet catalyst and gasoil temperatures are kept constant. The value of $\widetilde{E}_{net,max}$ varies significantly with the *H*/*D* riser ratio (between 0.15 and 0.35) which implies that this is an important variable to be considered in the thermodynamic optimization of the unit. As it is seen in Fig. 10, for *H*/*D* values between 10 and 20, the value of $\widetilde{E}_{net,max}$ increases rapidly with the increase of *H*/*D*. After this point, the value of $\widetilde{E}_{net,max}$ continues to increase with *H*/*D*, but at a small rate. The industrial riser units are normally built with *H*/*D* values varying between 30 and 40, which is in good agreement with the results shown in Fig. 10. It is also clear from Fig. 10 that increasing *H*/*D* above 40 will result only in a small increment in the available net exergy, and for constructive and economic reasons it might not even be feasible. The optimum values of COR for the maximum net exergy production are also presented in Fig. 10.

4. Conclusion

In the present work, an optimization methodology to be applied to FCC units was developed. The FCC risers mathematical model introduced by Souza et al. [15] combined with riser steady state experimental measurements available from SIX/PETROBRAS [16] was used to perform the FCC unit optimization study. The formulation uses a two-dimensional fluid flow solution which is not coupled with the kinetic and energy solutions. This simplifies the numerical solution, increasing convergence rates and decreasing computational time. Even though the velocity field is not exact, it is better than that obtained by the plug-flow approach and

improves the ability of the numerical code to determine the lumps mass fractions at the riser output section.

The results showed that the gasoline production can be maximized with respect to the catalyst/gasoil ratio (COR). It was verified that for any given catalyst mass flow rate, there exists an optimum value for the COR for maximum mass flow rate production of gasoline, or any other desired product. It was also introduced an exergy (thermodynamic) based optimization methodology for FCC units design. The process net exergy production rate was selected as the objective function for the optimization procedure, which in turn minimizes the system energetic losses.

The FCC unit thermodynamic optimization was based on the determination of the geometric parameters of the riser and the operating conditions of the unit for maximum thermodynamic performance. The objective function (net exergy production rate) was maximized through the minimization of the destroyed exergy inside the FCC unit. The optimization was conducted with respect to the catalyst to oil ratio (COR), and analyzing the sensitivity of the optima found with respect to the height to diameter riser ratio (H/D). It is important to stress that all optima are sharp, i.e., for example with $H/D = 50$, the variation of $\widetilde{E}_{\text{net}}$ is greater than 50%, calculated from $(\widetilde{E}_{\text{net,max}} - \widetilde{E}_{\text{net,min}})/\widetilde{E}_{\text{net,max}}$, for $5 < \text{COR} < 25$, which stresses their importance and utility for FCC unit design and operation. Based on the lack of second law analysis related works for FCC plants in the technical literature and in view of the potential gains suggested by the results, the authors believe that thermodynamic optimization could bring new insight in the quest for better FCC plants.

Acknowledgements

The authors acknowledge with gratitude the support of the Brazilian National Council of Scientific and Technological Development, CNPq, the Human Resources Program for the Oil and Natural Gas Sector at Federal University of Parana, Brazil, PRH-24/UFPR/ANP/MCT, the Brazilian Studies and Research Financier, through Project No. 1121/00-CTPETRO/FINEP, the SIX/PETROBRAS (Brazilian Oil Co.), and the Center for Advanced Power Systems at Florida State University, USA.

Appendix A. Model constitutive equations

The heat transfer rate terms used for the evaluation of the exergy rates are given by

$$\dot{Q}^{c}_{\text{cat}} = \dot{m}_{\text{cat}}\text{Cp}_{\text{cat}}\left(T_{\text{out}} - T^{\text{in}}_{\text{reg}}\right), \tag{A1}$$

$$\dot{Q}_{\text{cat}} = \dot{m}_{\text{cat}}\text{Cp}_{\text{cat}}\left(T^{\text{in}}_{\text{cat}} - T^{\text{in}}_{\text{reg}}\right), \tag{A2}$$

$$\dot{Q}_{\text{gasoil}} = \dot{m}_{\text{gasoil}}\text{Cp}_{\text{gasoil}}\left(T^{\text{in}}_{\text{gasoil}} - T_0\right), \tag{A3}$$

$$\dot{Q}_{\text{st}} = \dot{m}_w\text{Cp}_w(T^{\text{vap}}_w - T_0) + \dot{m}_w L_w + \dot{m}_{\text{st}}\text{Cp}_{\text{st}}\left(T^{\text{in}}_{\text{st}} - T^{\text{vap}}_{\text{st}}\right), \tag{A4}$$

$$\begin{aligned}\dot{Q}_{\text{prod}} = {} & (\dot{m}_{\text{vgo}} + \dot{m}_{\text{lco}} + \dot{m}_{\text{gsl}})\left[\text{Cp}^{\text{liq}}_{\text{cond}}(T^{\text{vap}}_{\text{cond}} - T_0) + L_{\text{cond}}\right. \\ & \left. + \text{Cp}^{v}_{\text{cond}}(T_{\text{out}} - T^{\text{vap}}_{\text{cond}})\right] + \dot{m}_{\text{LPG}}\text{Cp}^{v}_{\text{LPG}}(T_{\text{out}} - T_0) \\ & + \dot{m}_{\text{fg}}\text{Cp}^{v}_{\text{fg}}(T_{\text{out}} - T_0) + \dot{m}_{\text{coke}}\text{Cp}^{v}_{\text{coke}}(T_{\text{out}} - T_0),\end{aligned} \tag{A5}$$

$$\dot{Q}^{c}_{\text{st}} = \dot{m}_w\text{Cp}_w(T^{\text{vap}}_w - T_0) + \dot{m}_w L_w + \dot{m}_{\text{st}}\text{Cp}_{\text{st}}(T_{\text{out}} - T^{\text{vap}}_w), \tag{A6}$$

where c means cooling; in, inlet; out, outlet; vap, vaporization; cond, condensed; v, vapor phase; w, water; st, steam; 0 reference state; liq, liquid; lco, light cycle oil; gsl, gasoline; fg, fuel gas and LPG liquefied petroleum gas.

At the outlet section of the riser, a mixture of gases (steam, vgo, light cycle oil-lco, gasoline, LPG and fuel gas) leaves the FCC conversion unit. The water, vgo, lco and gasoline will then be condensed before they are ready for use. This cooling represents a loss of exergy and it is accounted for in the model by Eq. (41) with the constitutive Eq. (A5). It was assumed that the water and the hydrocarbons are immiscible.

In order to calculate the heat of vaporization of the hydrocarbon mixture (L_{cond}) the following procedure was applied.

First, the mass and molar fraction of the condensed mixture should be determined by

$$Y_i = \frac{\dot{m}_i}{\sum_j^4 \dot{m}_j}, \quad w_i = \frac{\dot{m}_i/M_i}{\sum_j^4 \dot{m}_j/M_j}, \tag{A7}$$

where w is the molar fraction, Y the mass fraction and j = vgo, lco and gasoline.

The vapor pressure for the mixture is calculated by the Antoine equation [28] given by

$$\log(P_{v,i}) = A_i - \frac{B_i}{T + C_i - 273.15}, \tag{A8}$$

where $P_{v,i}$ is the vapor pressure of component i and the dew temperature T.

The constants A, B and C were obtained from the work of Prausnitz et al. [28] assuming the lump/hydrocarbon equivalence presented in Table 2.

The molar fraction of the liquid phase for each mixture component is calculated by

$$w_i = \frac{PY_i}{P_{v,i}}, \tag{A9}$$

where P is the total pressure.

In the liquid phase, the sum of the molar fractions must be equal to one, thus:

$$1 = w_{\text{vgo}} + w_{\text{lco}} + w_{\text{gsl}}, \tag{A10}$$

where w_i is a function of P_{vi} and consequently a function of dew temperature.

Combining Eqs. (7)–(10) the dew temperature can be calculated.

The average boiling (T_b) and critical (T_c) temperature for the liquid phase are given by

$$T_b = w_{\text{vgo}}T_{b,\text{vgo}} + w_{\text{lco}}T_{b,\text{lco}} + w_{\text{gsl}}T_{b,\text{gsl}}, \tag{A11}$$

$$T_c = w_{\text{vgo}}T_{c,\text{vgo}} + w_{\text{lco}}T_{c,\text{lco}} + w_{\text{gsl}}T_{c,\text{gsl}}, \tag{A12}$$

In a similar form, the critical pressure is given by

$$P_c = w_{\text{vgo}}P_{c,\text{vgo}} + w_{\text{lco}}P_{c,\text{lco}} + w_{\text{gsl}}P_{c,\text{gsl}}, \tag{A13}$$

and the reduced temperature given by

$$T_{\text{br}} = \frac{T_b}{T_c}. \tag{A14}$$

The heat of vaporization can be expressed as [28]

$$L^0_{\text{cond}} = RT_cT_{\text{br}}\frac{3.987T_{\text{br}} - 3.958 + 1.555\ln(P_c)}{1.07 - T_{\text{br}}}. \tag{A15}$$

The dew temperature is different from the average boiling temperature (T_b) and for this reason it must be corrected by

$$L_{\text{cond}} = L^0_{\text{cond}}\left[\frac{(1 - T_{r2})}{(1 - T_{r1})}\right]^{0.38}, \tag{A16}$$

where

$$T_{r1} = \frac{T_b}{T_c}, \quad T_{r2} = \frac{T}{T_c}. \tag{A17}$$

For the water, the condensing temperature will be a function of its partial pressure which is calculated by

$$P_{v,w} = w_wP, \tag{A18}$$

where w_w is the molar fraction of water in the mixture.

References

[1] W. Krewitt, S. Teske, S. Simon, Energy [R]evolution 2008a sustainable world energy perspective, Energ. Policy 37 (12) (2009) 5764–5775.
[2] K.G. Satyanarayana, A.B. Mariano, J.V.C. Vargas, A review on microalgae, a versatile source for sustainable energy and materials, Int. J. Energ. Res., in press, doi:10.1002/er.1695.
[3] K.N. Theologos, N.C. Markatos, Advanced modeling of fluid catalytic cracking riser-type reactors, AIChE J. 39 (6) (1993) 1007–1017.
[4] J.S. Gao, C.M. Xu, S.X. Lin, G.H. Yang, Y.C. Guo, Simulations of gas–liquid–solid 3-phase flow and reaction in FCC riser reactors, AIChE J. 47 (3) (2001) 677–692.
[5] I.S. Han, C.B. Chung, Dynamic modeling and simulation of a fluidized catalytic cracking process. Part I: process modeling, Chem. Eng. Sci. 56 (5) (2001) 1951–1971.
[6] W.P. Martignoni, Modelling and simulation of FCC riser reactors: a heterogeneous approach, Ph.D. Thesis, University of Western Ontario, Ontario, Canada, 1998.
[7] I.S. Han, J.B. Riggs, C.B. Chung, Modeling and optimization of a fluidized catalytic cracking process under full and partial combustion modes, Chem. Eng. Process. 43 (8) (2004) 1063–1084.
[8] J.A. Souza, Numerical simulation and thermodynamic optimization of fluidized catalytic cracking risers for maximizing fuel production, Ph.D. Thesis, Federal University of Parana, Curitiba, PR, Brazil (in Portuguese), 2004.
[9] J.A. Souza, J.V.C. Vargas, O.F. von Meien, W.P. Martignoni, J.C. Ordonez, The inverse methodology of parameter estimation for model adjustment, design, simulation, control and optimization of fluid catalytic cracking (FCC) risers, J. Chem. Technol. Biotechnol. 84 (2009) 343–355.
[10] R.B. Kasat, D. Kunzru, D.N. Saraf, S.K. Gupta, Multiobjective optimization of industrial FCC units using elitist non-dominated sorting genetic algorithm, Ind. Eng. Chem. Res. 41 (2002) 4765–4776.
[11] R.C. Ellis, X. Li, J.B. Riggs, Modeling and optimization of a model IV fluidized catalytic cracking unit, AIChE J. 44 (1998) 2068–2079.
[12] C.M. Song, Z.F. Yan, Y.S. Tu, Energy and exergy analysis of FCC unit, Abstr. Pap. Am. Chem. Soc. 217 (1999) U805.
[13] A. Bejan, Advanced Engineering Thermodynamics, Wiley, New York, 1987.
[14] A. Bejan, G. Tsatsaronis, M.J. Moran, Thermal Design and Optimization, Wiley, New York, 1996.
[15] J.A. Souza, J.V.C. Vargas, O.F. von Meien, W.P. Martignoni, S.C. Amico, A simplified two-dimensional model for the simulation, control and optimization of FCC risers, AIChE J. 52 (5) (2006) 1895–1905.
[16] Petrobras Six, Riser Improvement Project, Internal Report (in Portuguese), São Mateus do Sul, PR, Brazil, 2001.
[17] N. Zabaras, Inverse problems in heat transfer, in: W.J. Minkowycz, E.M. Sparrow, G.E. Schneider, R.H. Pletcher (Eds.), Handbook of Numerical Heat Transfer, second ed., Wiley, New York, 2006, pp. 525–558. Chapter 17.
[18] H. Ali, S. Rohani, Dynamic modeling and simulation of a riser-type fluid catalytic cracking unit, Chem. Eng. Technol. 20 (1997) 118–130.
[19] W.P. Martignoni, H.I. Lasa, Heterogeneous reaction model for FCC riser units, Chem. Eng. Sci. 56 (2001) 605–612.
[20] Petrobras Six, List of Kinetic Parameters and Arrhenius Constants for the 6-lump Model, Internal Report (in Portuguese), São Mateus do Sul, PR, Brazil, 2001.
[21] J. Ancheyta-Juárez, J.A. Murillo-Hernández, A simple method for estimating gasoline, gas, and coke yields in FCC Process, Energ. Fuel 14 (2000) 373–379.
[22] A. Miller, D. Gidaspow, Dense, vertical gas–solid flow in a pipe, AIChE J. 38 (1992) 1801–1815.
[23] V.K. Areek, A.A. Adesina, A. Srivastava, R. Sharmar, Modeling of a nonisothermal FCC riser, Chem. Eng. J. 92 (2003) 101–109.
[24] J. Gao, C. Xu, S. Lin, G. Yang, Advanced model for turbulent gas–solid flow and reaction in CC riser reactors, AIChE J. 45 (1999) 1095–1113.
[25] J. Gao, C. Xu, S. Lin, G. Yang, Simulations of gas–liquid–solid 3-phase flow and reaction in FCC riser reactors, AIChE J. 47 (2001) 667–692.
[26] J.V.C. Vargas, G. Stanescu, R. Florea, M.C. Campos, A numerical model to predict the thermal and psychometric response of electronic packages, J. Electron. Packag. 123 (2001) 200–210.
[27] R.H. Perry, D.W. Green, Chemical Engineers' Handbook, eighth ed., McGraw-Hill, New York, 2008.
[28] J. Prausnitz, B.E.M. Poling, J.P. O'Connell, The Properties of Gases and Liquids, fifth ed., McGraw-Hill, New York, 2001.